

## Supplementary Material

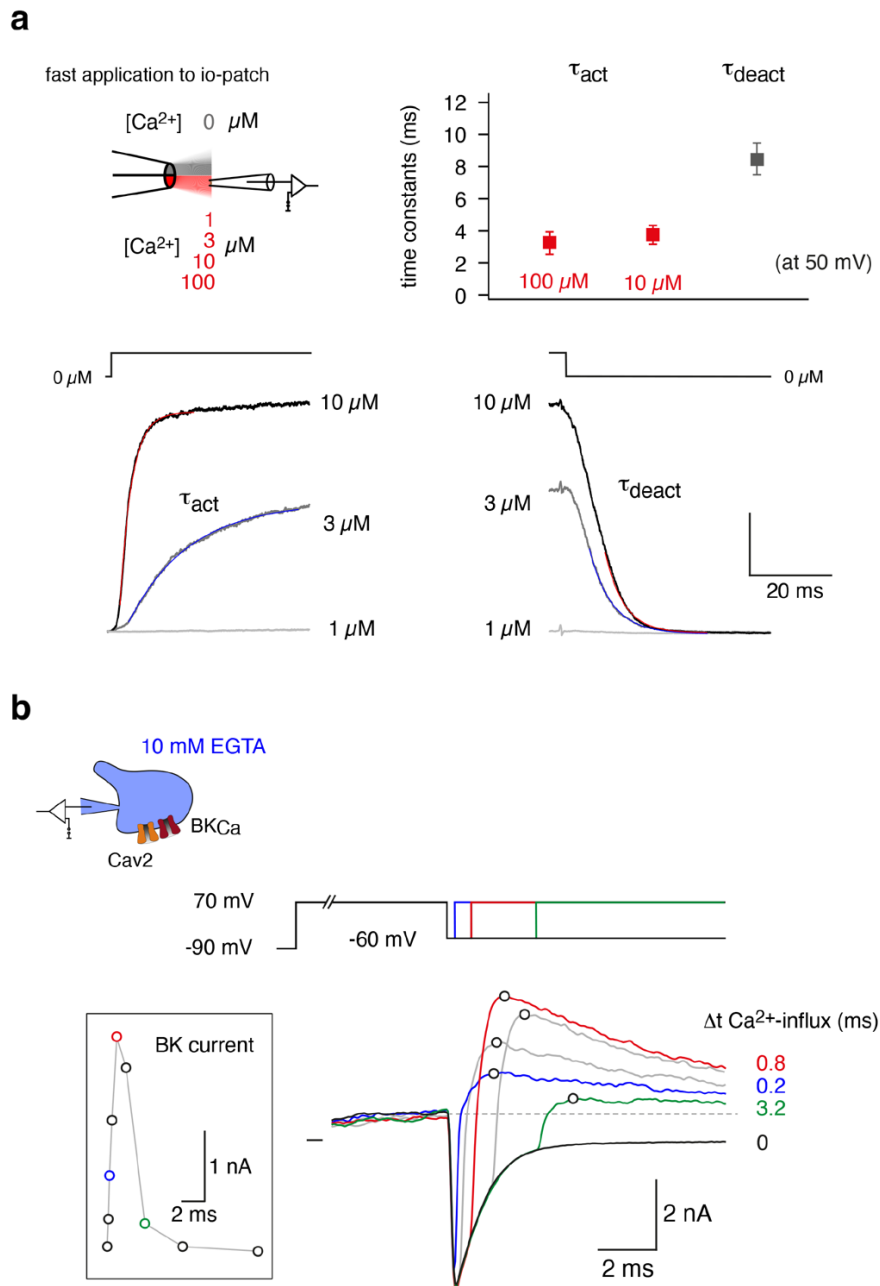
### Ca<sup>2+</sup>-pumping by PMCA-Neuroplastin complexes operates in the kiloHertz-range

Cristina E. Constantin, Barbara Schmidt, Yvonne Schwarz, Harumi Harada,  
Astrid Kollwe, Catrin S. Müller, Sebastian Henrich, Botond Gaal, Akos Kulik,  
Dieter Bruns, Uwe Schulte, Heiko Rieger and Bernd Fakler

- Supplementary Figures 1 - 5
- Supplementary Tables 1 - 3

## Supplementary Figures

### Supplementary Figure 1 (information related to Figure 1)



### Supplementary Figure 1

#### Ca<sup>2+</sup>-gating of BK<sub>Ca</sub> channels

**a**, Activation and deactivation of BK<sub>Ca</sub> channels determined at a membrane potential of 50 mV with a piezo-driven fast-application system exchanging [Ca<sup>2+</sup>]<sub>i</sub> at the cytoplasmic face of the channels in the sub-millisecond range (termed: Ca<sup>2+</sup>-gating<sup>23</sup>). Upper left panel: Scheme of the fast-application system exchanging solutions with the indicated values for [Ca<sup>2+</sup>]<sub>i</sub> and a Ca<sup>2+</sup>-free solution. Upper right panel: Values for activation and deactivation time constants of Ca<sup>2+</sup>-gating at 50 mV. Lower panel: Representative current responses of BK<sub>Ca</sub> channels to either an increase in [Ca<sup>2+</sup>]<sub>i</sub>

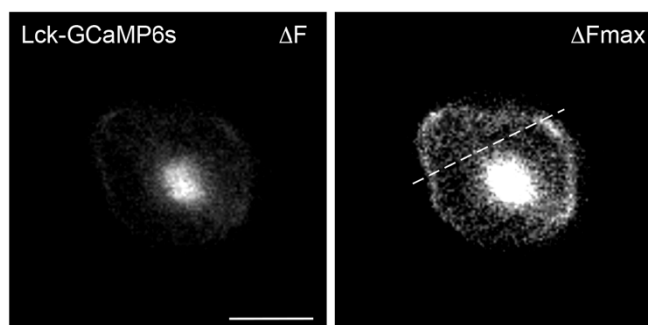
(from 0 to 1, 3 or 10  $\mu\text{M}$  (left) or a decrease in  $[\text{Ca}^{2+}]_i$  (from 1, 3 and 10  $\mu\text{M}$  to 0 (right)). Lines represent fits of a mono-exponential function to the activation and deactivation phases with time constants of 2.8 ms (red) and 14.7 ms (blue) for activation at 10 and 3  $\mu\text{M}$   $\text{Ca}^{2+}$ , respectively, and 6.0 ms (red) and 5.3 ms (blue) for deactivation from 10 and 3  $\mu\text{M}$   $\text{Ca}^{2+}$ , respectively. Time scale as indicated, current scale is 0.5 nA. (Data were taken from <sup>23</sup>).

**b**, Current responses (color-coded) recorded in a CHO cell with the indicated voltage-protocol, protein expression and ion conditions were identical to the experiments in Fig. 1c, the patch pipette contained 10 mM EGTA. Trace in black reflects the  $\text{Ca}^{2+}$ -inward current through Cav2.2 channels (following step-repolarization from 70 mV to -60 mV), while colored traces highlight  $\text{BK}_{\text{Ca}}$ -mediated outward  $\text{K}^+$  currents as in Fig. 1c activated by  $\text{Ca}^{2+}$ -influx of 0.2 ms (blue), 0.8 ms (red) and 3.2 ms (green) duration, as well as by  $\text{Ca}^{2+}$ -influx of 0.4 and 1.6 ms (light grey, for better discrimination).

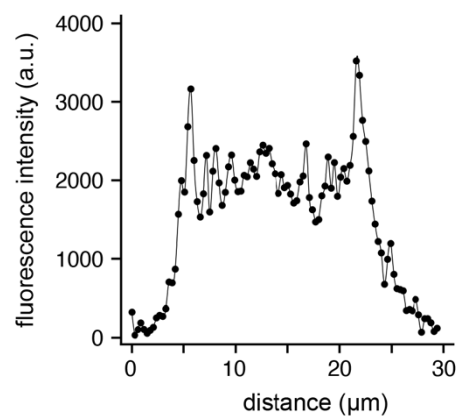
Note the accurate monitoring of  $[\text{Ca}^{2+}]_i$  by the  $\text{BK}_{\text{Ca}}$ -current maximum. Scaling for time and current as indicated, dashed line denotes  $\text{BK}_{\text{Ca}}$ -current prior to  $\text{Ca}^{2+}$ -influx, small line is zero current.

## Supplementary Figure 2 (information related to Figure 1)

**a**



**b**



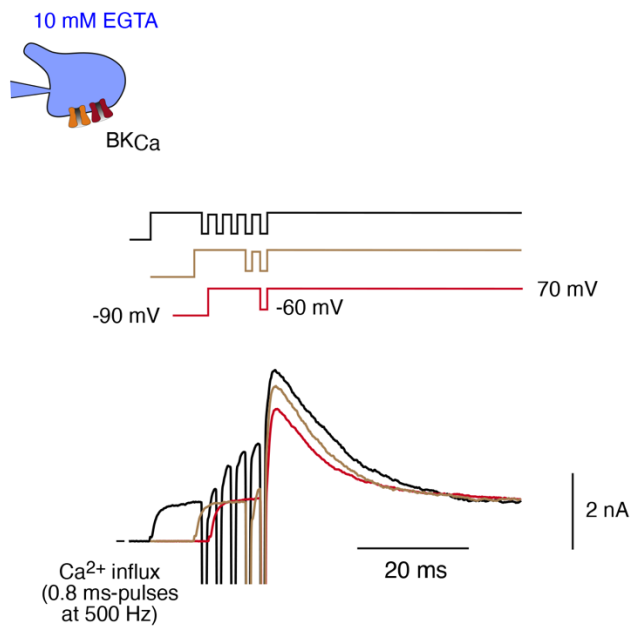
## Supplementary Figure 2

### Fluorescence measurements by membrane-tethered GCaM6s

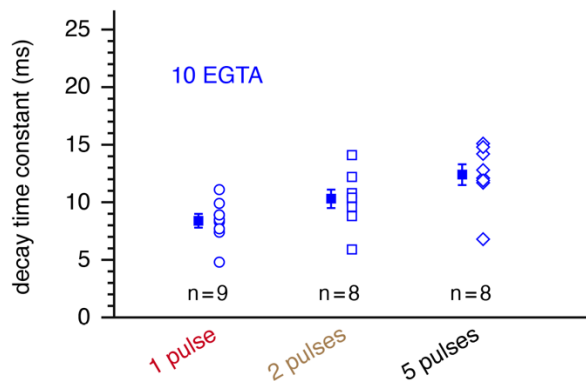
**a**, Representative image of a CHO cell expressing Lck-GCaM6s before (left panel) and during/after step stimulation (right panel) with the voltage protocol in Fig. 1e. Dashed line is line-scan used for fluorescence measurement. **b**, Fluorescence intensity obtained along the line in (a).

## Supplementary Figure 3 (information related to Figure 1)

**a**



**b**



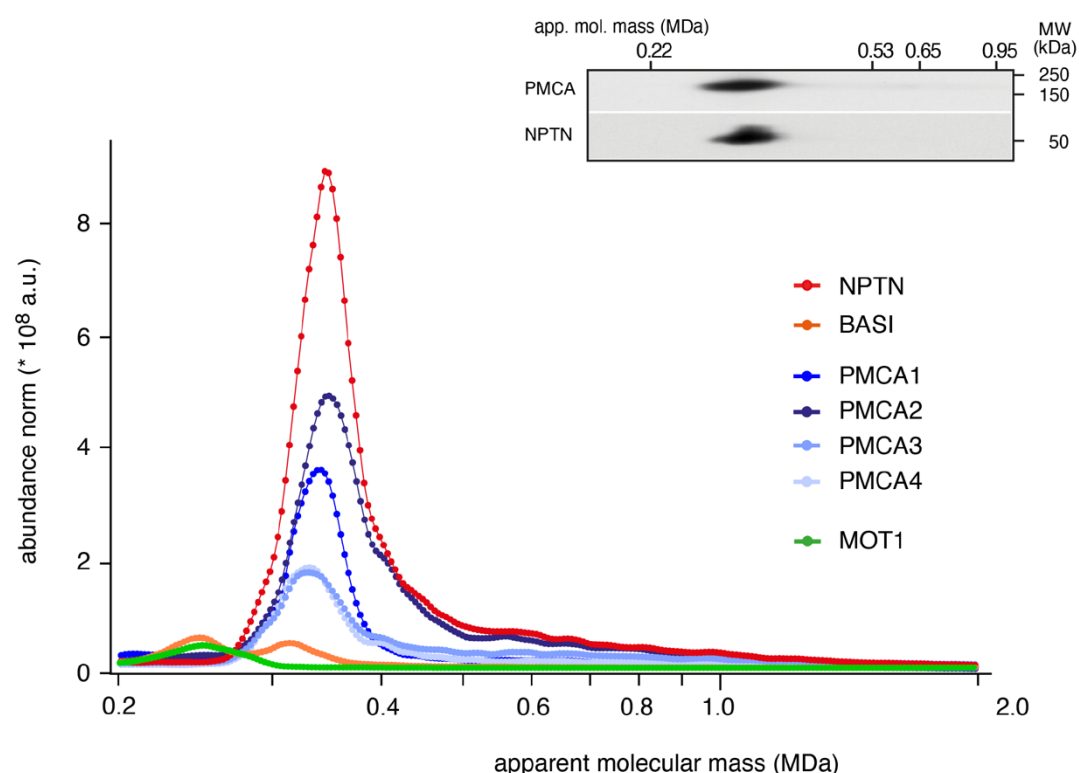
## Supplementary Figure 3

### Ca<sup>2+</sup>-clearance by 10 mM EGTA in pulse-experiments

**a**, Representative BK<sub>Ca</sub>-currents recorded in response to 1, 2 and 5 Ca<sup>2+</sup>-influx pulses applied at 500 Hz (voltage protocol in lower inset) to CHO cells as in Figure 1, but with 10 mM EGTA in the patch-pipette (upper inset). **b**, Plot summarizing the time constants of the current decay determined in experiments as in (**a**); squares represent mean  $\pm$  SEM of the indicated number of cells.

## Supplementary Figure 4 (information related to Figure 2)

csBN-MS, mouse brain membranes

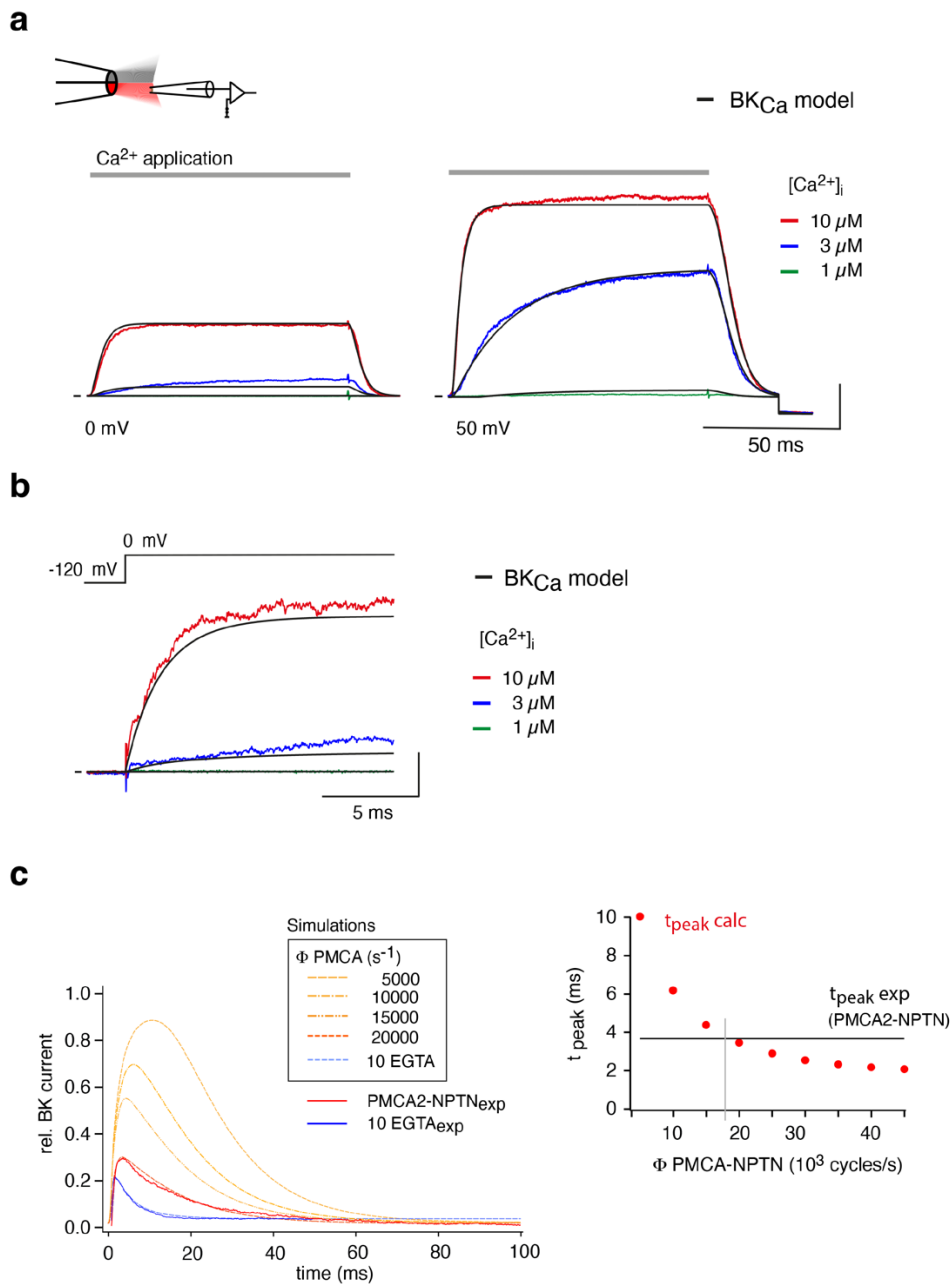


## Supplementary Figure 4

### Abundance-mass profiles of the constituents of native PMCA complexes in the mouse brain

Abundance-mass profiles obtained by cryo-slicing BN-MS (csBN-MS, <sup>50</sup>) for the indicated proteins in a CL-47 solubilized membrane fractions from adult mouse brain (a total of 170 gel slices). Note the co-segregation of all PMCA isoforms with NPTN and a sub-population of BASI. The other sub-population of BASI co-assembles with the mono-carboxylate-transporter MOT1. Inset: Two-dimensional gel separation of PMCA1-4 and NPTN in the same membrane fractions, Western-probed with antibodies targeting PMCA1-4 and NPTN. Size (BN-PAGE) and molecular weight (SDS-PAGE) are as indicated.

## Supplementary Figure 5 (information related to Figure 3)



## Supplementary Figure 5

### Calibration of the gating model of BK<sub>Ca</sub> channels

**a, b** Calibration of the extended BK<sub>Ca</sub>-model via parameter-fitting to the BK<sub>Ca</sub>-mediated currents recorded in experiments as in Extended Data Figure 1 (data taken from <sup>23</sup>). BK<sub>Ca</sub>-currents were elicited by fast application of solutions with the indicated [Ca<sup>2+</sup>]<sub>i</sub> at the indicated constant membrane potential (**a**, Ca<sup>2+</sup>-gating), or by the indicated voltage-step with the indicated [Ca<sup>2+</sup>]<sub>i</sub> constantly present at the cytoplasmic face of the channels (**b**, voltage-gating). Black lines represent the response of the BK<sub>Ca</sub>-model to the respective changes in [Ca<sup>2+</sup>]<sub>i</sub> and membrane potential. Note the good approximation of the experimental data by the calibrated model (parameters of the gating model are given in Supplementary Table 3).

**c**, Dependence of the time-to-peak ( $t_{\text{peak}}$ ) of the  $\text{BK}_{\text{Ca}}$ -current maximum on the transport rate of the PMCA2-NPTN pumps (right panel) obtained from the calculations in Figure 3 (left panel). Note that perfect match between experimentally measured  $t_{\text{peak}}$  (black line,  $t_{\text{peak exp}}$  (right panel) or current trace in red (left panel)) and calculated  $t_{\text{peak}}$  ( $t_{\text{peak calc}}$ ) is observed at a transport rate of about 18.000/s (grey line, right panel).

## Supplementary Tables

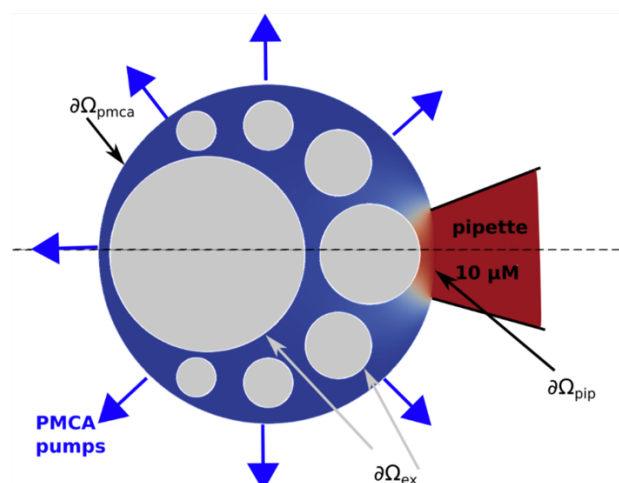
### Supplementary Table 1.

Parameters defining model cell and spatio-temporal profiles for intracellular  $\text{Ca}^{2+}$  concentration.

parameter	value	description
$C_0$	0.1 $\mu\text{M}$ [1]	$[\text{Ca}^{2+}]$ at rest
$D_c$	0.22 $\mu\text{m}^2/\text{ms}$ [1]	$\text{Ca}^{2+}$ diffusion constant
$r$	5 $\mu\text{m}$	cell radius
$r_{\text{pip}}$	1.25 $\mu\text{m}$	pipette radius
$C_{\text{pip}}$	10 $\mu\text{M}$	$[\text{Ca}^{2+}]$ at pipette
$P_{\text{PMCA}}$	50/ $\mu\text{m}^2$ [2]	surface density of PMCA-NTPN
$C_{1/2}$	0.43 $\mu\text{M}$ [3]	Hill parameter
$n$	2 [3]	Hill coefficient
$\Phi_{\text{PMCA}}$	free parameter	PMCA pump strength
$b_t$	0 or 10 mM [2]	total amount of [EGTA]
$D_b$	0.113 $\mu\text{m}^2/\text{ms}$	EGTA diffusion constant
$b_{\text{pip}}$	0 or 10 mM [2]	[EGTA] at pipette
$k_+$	2.55 / $\mu\text{Ms}$ [1]	on-rate for $\text{Ca}^{2+}$ -EGTA binding
$k_-$	0.45/s [1]	off-rate for $\text{Ca}^{2+}$ -EGTA binding
$N_{\text{CaV}}$	1.200 000 [2]	number of incoming $\text{Ca}^{2+}$
$\Delta t$	0.8 ms [2]	duration of the voltage pulse

#### References

- [1] citation 32
- [2] this study
- [3] citation 54



#### Equatorial cross-section of the spherically shaped model geometry

The three-dimensional geometry is generated by rotating this cross section around its symmetry axis indicated by the straight dashed line. The outer boundary  $\partial\Omega$  of the cell volume  $\Omega$  is partitioned into  $\partial\Omega_{\text{pmca}}$  comprising PMCA, Cav and leak  $\text{Ca}^{2+}$  currents, and  $\partial\Omega_{\text{pip}}$  with pipette solution-defined fixed  $\text{Ca}^{2+}$  concentration. Grey regions denote cross sections of intracellular organelles whose volumes are inaccessible to diffusing  $\text{Ca}^{2+}$  (70% of total intracellular volume), the boundaries,  $\partial\Omega_{\text{ex}}$ , of these excluded sub-volumes have no-flux boundary conditions for  $\text{Ca}^{2+}$  diffusion.

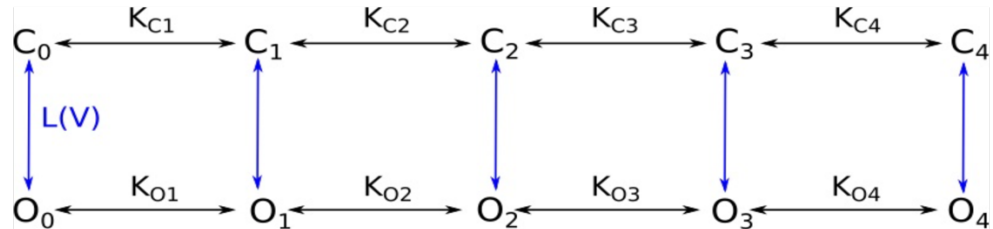


## Supplementary Table 2.

Parameters defining the  $BK_{Ca}$ -gating model used for computing the response to stationary conditions in  $[Ca^{2+}]_i$ .

parameter value

Q	0.94 e
$K_{C1}$	27.1 $\mu M$
$K_{C2}$	0.09 $\mu M$
$K_{C3}$	8.57 $\mu M$
$K_{C4}$	7.74 $\mu M$
$L(0)$	80.5
$K_{O1}$	15.08 $\mu M$
$K_{O2}$	0.06 $\mu M$
$K_{O3}$	0.6 $\mu M$
$K_{O4}$	4.29 $\mu M$



**Stationary gating scheme for  $BK_{Ca}$  channels** (adapted and modified from (30)).

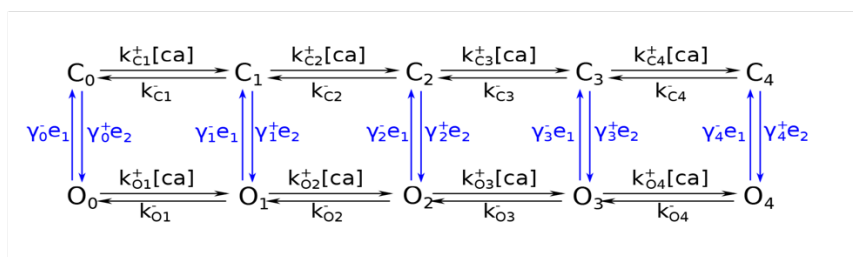
Voltage dependent rates  $L(V) = L(0) \cdot \exp(-QFV/RT)$  define the transition between open and closed conformation, where  $L(0)$  is the open-to-closed equilibrium constant in the absence of bound  $Ca^{2+}$  at 0 mV,  $V$  is transmembrane voltage,  $Q$  is equivalent gating charges associated with the closed-to-open conformational change and  $R$ ,  $T$ ,  $F$  have their usual meaning.  $K_{Ci}$  and  $K_{Oi}$  define binding of  $Ca^{2+}$  to the four binding sites of  $BK_{Ca}$  (used in eq. 7)

## Supplementary Table 3.

Parameters defining the extended  $BK_{Ca}$ -gating model used for computing the response to pulsed increases in  $[Ca^{2+}]_i$ .

parameter value parameter value

$\gamma_0^+$	1/18.03 s	$\gamma_0^-$	1/0.0009 s
$\gamma_1^+$	1/80.02 s	$\gamma_1^-$	1/0.016 s
$\gamma_2^+$	1/0.98 s	$\gamma_2^-$	1/0.0012 s
$\gamma_3^+$	1/0.008 s	$\gamma_3^-$	1/0.00016 s
$\gamma_4^+$	1/0.006 s	$\gamma_4^-$	1/0.002 s
$Q_1$	2.25e	$Q_2$	-0.11e
$k_{C1}^+$	34.1/ $\mu Ms$	$k_{C1}^-$	1741.68/s
$k_{C2}^+$	3972.8/ $\mu Ms$	$k_{C2}^-$	1015.79/s
$k_{C3}^+$	208.92/ $\mu Ms$	$k_{C3}^-$	20617.6/s
$k_{C4}^+$	711.2/ $\mu Ms$	$k_{C4}^-$	4449.017/s
$K_{O1}^+$	537.19/ $\mu Ms$	$K_{O1}^-$	7536.7/s
$K_{O2}^+$	727.16/ $\mu Ms$	$K_{O2}^-$	29.81/s
$K_{O3}^+$	32.63/ $\mu Ms$	$K_{O3}^-$	20.9/s
$K_{O4}^+$	314.8/ $\mu Ms$	$K_{O4}^-$	121.1/s



**Gating scheme for  $BK_{Ca}$  - non stationary case** (adapted and modified from (30)).

Voltage-dependent transition rates are defined as  $e_1(V) = \exp(Q_1 FV/RT)$  and  $e_2(V) = \exp(Q_2 FV/RT)$ , with  $V$  being transmembrane voltage and  $R$ ,  $T$ ,  $F$  and  $Q_i$  as in Supplementary Table 2.